

See discussions, stats, and author profiles for this publication at: <https://www.researchgate.net/publication/221729146>

# Hybrid density functional/molecular mechanics studies on activated adsorption of oxygen on zeolite supported gold monomer

ARTICLE *in* THE JOURNAL OF CHEMICAL PHYSICS · DECEMBER 2011

Impact Factor: 2.95 · DOI: 10.1063/1.3667206 · Source: PubMed

---

CITATIONS

2

---

READS

33

## 2 AUTHORS:



**Subhi Baishya**

Tezpur University

4 PUBLICATIONS 10 CITATIONS

SEE PROFILE



**Ramesh C Deka**

Tezpur University

99 PUBLICATIONS 1,011 CITATIONS

SEE PROFILE

## Hybrid density functional/molecular mechanics studies on activated adsorption of oxygen on zeolite supported gold monomer

Subhi Baishya and Ramesh C. Deka

Citation: *J. Chem. Phys.* **135**, 244703 (2011); doi: 10.1063/1.3667206

View online: <http://dx.doi.org/10.1063/1.3667206>

View Table of Contents: <http://jcp.aip.org/resource/1/JCPSA6/v135/i24>

Published by the [American Institute of Physics](#).

---

### Related Articles

Modeling intermolecular interactions of physisorbed organic molecules using pair potential calculations

*J. Chem. Phys.* **135**, 234703 (2011)

Adsorption and dissociation of NO on Ir(100): A first-principles study

*J. Chem. Phys.* **135**, 204707 (2011)

Combined optical and acoustical method for determination of thickness and porosity of transparent organic layers below the ultra-thin film limit

*Rev. Sci. Instrum.* **82**, 103111 (2011)

Communication: Lateral phase separation of mixed polymer brushes physisorbed on planar substrates

*J. Chem. Phys.* **135**, 141106 (2011)

Extension of the Steele 10-4-3 potential for adsorption calculations in cylindrical, spherical, and other pore geometries

*J. Chem. Phys.* **135**, 084703 (2011)

---

### Additional information on *J. Chem. Phys.*

Journal Homepage: <http://jcp.aip.org/>

Journal Information: [http://jcp.aip.org/about/about\\_the\\_journal](http://jcp.aip.org/about/about_the_journal)

Top downloads: [http://jcp.aip.org/features/most\\_downloaded](http://jcp.aip.org/features/most_downloaded)

Information for Authors: <http://jcp.aip.org/authors>

### ADVERTISEMENT



**AIP**Advances

*Submit Now*

**Explore AIP's new  
open-access journal**

- **Article-level metrics  
now available**
- **Join the conversation!  
Rate & comment on articles**

# Hybrid density functional/molecular mechanics studies on activated adsorption of oxygen on zeolite supported gold monomer

Subhi Baishya and Ramesh C. Deka<sup>a)</sup>

Department of Chemical Sciences, Tezpur University, Napaam 784028, India

(Received 15 September 2011; accepted 18 November 2011; published online 23 December 2011)

Density functional theory calculations on oxygen adsorption over gas phase and faujasite supported Au monomer has been studied using hybrid quantum mechanics/molecular mechanics method, surface integrated molecular orbital molecular mechanics implemented in GAMESS package. Three different oxidation states of Au (0, +1, +3) and three different adsorption modes viz., top, bridge, and dissociative adsorption of oxygen have been considered in our calculations. Redshift in the  $\nu_{O-O}$  value from that in gas phase  $O_2$  indicates activation of  $O_2$  upon adsorption over faujasite supported gold monomer. The activation of  $O_2$  is an important step in the catalytic oxidation of CO. The presence of adsorbed  $O_2$  increases the interaction of the Au monomer with the faujasite support. In faujasite supported cationic Au monomer,  $O_2$  preferably remains bridge bonded to Au rather than being dissociated. © 2011 American Institute of Physics. [doi:10.1063/1.3667206]

## I. INTRODUCTION

Nanosized materials differ considerably from the bulk material and have drawn much attention from the past decade owing to the unique reactive behavior. Studies have been devoted to both supported and unsupported nanosized metal clusters and their catalytic applications. Bulk gold is inert, but effectively catalyzes the low temperature CO oxidation on reducing the dimensions.<sup>1–3</sup> Apart from the CO oxidation reaction, other reactions being catalyzed include water-gas shift (WGS) reaction,<sup>4</sup> chemoselective hydrogenation,<sup>5</sup> and selective oxidation of olefins,<sup>6,7</sup> etc. However, to gain insight into the catalytic mechanism of the CO oxidation reaction, oxygen adsorption behavior on gold clusters is necessary. The reaction of  $O_2$  molecule with metal clusters of various sizes is specifically important as it can help to identify a potential catalyst for oxidation reactions. Pioneering experimental works on the adsorption of oxygen molecule on Au cluster anions by Cox *et al.*<sup>8,9</sup> showed a dramatic even-odd oscillation in the reactivity with only even atom cluster anions (i.e., those with odd number of electrons) exhibiting the adsorption of one  $O_2$  molecule. It has also been found that odd cluster anions exhibit negligible or very little adsorption and that anionic gold clusters cannot bind two  $O_2$  molecules. However, their work indicated no activity of neutral and cationic Au clusters toward  $O_2$  molecule except  $Au_{10}^+$  cluster. Low temperature activity studies of molecular oxygen on gold cluster anions by Salisbury *et al.*<sup>10</sup> showed the adsorbed oxygen to be oxygen molecule instead of O,  $O_3$  adsorption or co-adsorption of two  $O_2$  molecules. Studies by different groups<sup>8–14</sup> generalized that the adsorption strength of  $O_2$  is greatest in anionic gold clusters although adsorption has been observed on neutral and rarely on cationic clusters. An important experimental outcome is that  $O_2$  can interact better with Au clusters having odd number of electrons and that anionic Au clusters with

even number of Au atoms adsorb one  $O_2$  easily while those with odd Au atoms showed no or very little adsorption. Density functional theory (DFT) study by Mills *et al.*<sup>15</sup> on  $O_2$  binding to Au clusters and Au(111) surface modified by adsorption of Au clusters on it predicted that binding of  $O_2$  is strong when the number of electrons is odd and hence all anionic gold clusters adsorb  $O_2$  molecule. Ding *et al.*<sup>16</sup> studied the adsorption properties of  $O_2$  molecule on anionic, cationic, and neutral  $Au_n$  clusters ( $n = 1–6$ ) using B3LYP functional. Their work predicted the binding energy of  $O_2$  to cationic gold clusters to be very small ( $<0.5$  eV) and in the case of neutral clusters,  $Au_5$  can adsorb one  $O_2$  molecule while  $Au_3$  can weakly adsorb up to two  $O_2$  molecules. In addition to these, a number of theoretical studies<sup>17–24</sup> have been made mostly on the adsorption of  $O_2$  on anionic clusters, but studies on neutral and cationic clusters are really scarce.

Gold dispersed on solid support forms an important class of catalyst due to their unique catalytic property. Zeolites, owing to their ability to disperse gold, because of the internal distribution of the pores and the ability to control particle size, form a very promising type of support for gold nanoparticles. Zeolites also possess adjustable acidic properties and have pores and cavities of molecular dimensions.  $Au^+$  species dispersed inside NaY and ZSM-5 zeolites has been shown to exhibit high activity for CO and NO chemisorption as well as direct NO decomposition reactions.<sup>25–27</sup> The  $Au^0$  and  $Au^+$  sites in Au supported on ZSM-5 and mordenite have been considered responsible for low temperature CO oxidation and the water-gas shift reaction.<sup>28,29</sup> Different experimental works<sup>30–34</sup> have been reported for determining the active sites in gold/zeolite support system for the CO oxidation reaction and  $Au^+$ ,  $Au^{3+}$ , or  $Au_n^{\delta+}$  or neutral  $Au_n$  have been proposed to be the reactive sites for the reaction depending on reaction condition. Despite many experimental findings, studies related to the mechanistic determination of the CO oxidation reaction remain unattempted. The dissociative mode of  $O_2$  adsorption on single gold crystals has been

<sup>a)</sup> Author to whom correspondence should be addressed. Electronic mail: ramesh@tezu.ernet.in.

considered energetically unfavorable but various theoretical calculations have proposed the ability of low coordinated gold atoms to adsorb and dissociate  $O_2$ .<sup>15,35–37</sup> A recent study has been made by Boronat and Corma<sup>38</sup> on  $O_2$  activation on different gold surfaces and nanoparticles to separate the effect of particle size, morphology, and support and found that  $O_2$  is most activated in the bridge–bridge conformation with lowest barrier for  $O_2$  activation. In the case of gold particles supported on  $TiO_2$ , the metal-support interface has been found to be the most stable sites for  $O_2$  adsorption and the most active sites for  $O_2$  dissociation. Their work demonstrated that  $O_2$  dissociation is sensitive to the structure of gold surface. While theoretical studies about gold supported on oxides such as  $MgO$ ,  $TiO_2$ , and  $Al_2O_3$  are found, but studies on gold/zeolite supported system is very limited. One of the key factors to understand the details of CO oxidation reaction on gold/zeolite support system is the adsorption of  $O_2$ . Also it is necessary to understand the change in adsorption behavior with change in the charge state of gold. Gold exhibits varying oxidation states when supported on zeolite depending on the Si/Al ratio. Substitution of a framework Si atom with an Al atom creates an excess negative charge which can be compensated by the inclusion of an extra framework Au atom. To the best of our knowledge, no theoretical studies have been reported on the adsorption of  $O_2$  on faujasite supported Au monomer. It will be quite interesting to study the  $O_2$  adsorption on faujasite supported Au in different charge states, 0, +1, +3 and hence compare the results with the gas phase counterparts. We have considered possible three different modes of  $O_2$  adsorption viz., top mode in which one oxygen atom is directly bonded to Au, bridging mode with  $O_2$  chelating Au, and dissociative mode in which  $O_2$  adsorbs in a dissociative manner.

## II. COMPUTATIONAL METHOD

Hybrid quantum mechanics/molecular mechanics method SIMOMM (surface integrated molecular orbital molecular mechanics) (Ref. 39) implemented in GAMESS has been used to carry out the calculations. The zeolite model employed in this work comprises of 642 atoms and an extra framework Au atom (Fig. 1). In the SIMOMM method, the entire system is divided into two regions: the chemically active part which is treated quantum mechanically and the outer inactive part, modeled using molecular mechanics. In our system the quantum mechanical part comprises of a six membered ring of the faujasite zeolite and an Au atom supported on it along with the adsorbed  $O_2$  molecule. This quantum mechanical part is treated with the DFT based B3LYP functional and 6–31 G basis set for Si, Al, O, and H while LANL2DZ basis set incorporating relativistic effective core potential for Au atom. On the other hand, the outer region is modeled using the MM3 parameter. The binding energy for the  $O_2$  molecule is calculated using:

$$\text{B.E.}(O_2 \text{ on gas phase Au}) = (E_{Au} + E_{O_2}) - E_{Au-O_2}, \quad (1)$$

$$\begin{aligned} \text{B.E.}(O_2 \text{ on zeolite supported Au}) = & (E_{Au/FAU} + E_{O_2}) \\ & - E_{Au-O_2/FAU}. \end{aligned} \quad (2)$$

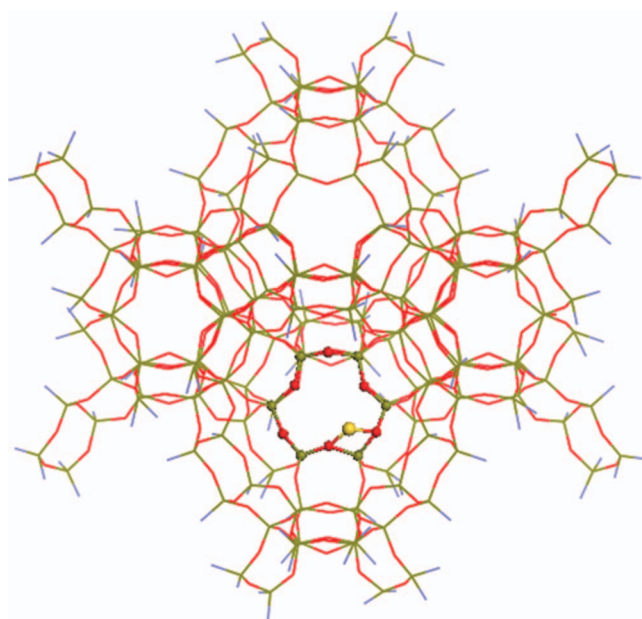


FIG. 1. Faujasite model used in the calculations, the QM part has been shown by ball and stick and the MM part by line. Gray—H, red—O, green—Si, and yellow—Au.

Natural bond orbital (NBO) analysis has been performed using GAUSSIAN09 program package<sup>40</sup> in order to investigate the nature of interaction between the gold atom and oxygen molecule.

## III. RESULTS AND DISCUSSION

### A. $O_2$ adsorption over gas phase Au monomer

The triplet oxygen found to be more stable has been considered in our calculations. Considering the top mode of coordination (Fig. 2(a)), when  $O_2$  was adsorbed on gas phase Au atom, the binding energy is found to decrease with increase in oxidation state, i.e., from  $Au^0$  to  $Au^+$ . For  $Au^0$ , the binding energy is found to be 0.26 eV while for  $Au^+$ ; the  $O_2$  binding becomes quite unfavorable evident from the negative binding energy value of  $-0.42$  eV. However, no adsorption of  $O_2$  on  $Au^{3+}$  was found. Electron transfer from  $Au^0$  to  $O_2$  accompanying  $O_2$  adsorption populates the  $\pi^*$  antibonding orbital of  $O_2$ , thus decreasing the O–O bond order.  $O_2$  thus reduces to superoxide evident from the elongated O–O bond length of 1.33 Å (1.25 Å in gas phase  $O_2$ ) indicating  $O_2$  activation upon adsorption on neutral gold atom. However, in the case of  $O_2$  adsorption on cationic gold, i.e., on  $Au^+$ , the O–O bond length remains the same as that in  $O_2$  molecule (1.25 Å in  $Au^+-O_2$  as against 1.25 Å in  $O_2$ ). In other words, the O–O bond is not activated when adsorbed on  $Au^+$  indicating that the interaction here is mostly electrostatic. The variation in O–O bond length is also accompanied by the corresponding change in O–O vibrational frequency with the smallest value for the longest O–O bond length. The  $\nu_{O-O}$  value is found to be  $1067.1 \text{ cm}^{-1}$  for the neutral Au which increases to  $1441.6 \text{ cm}^{-1}$  for  $Au^+$ . Referring to Au–O bond, the bond length is 2.21 Å in



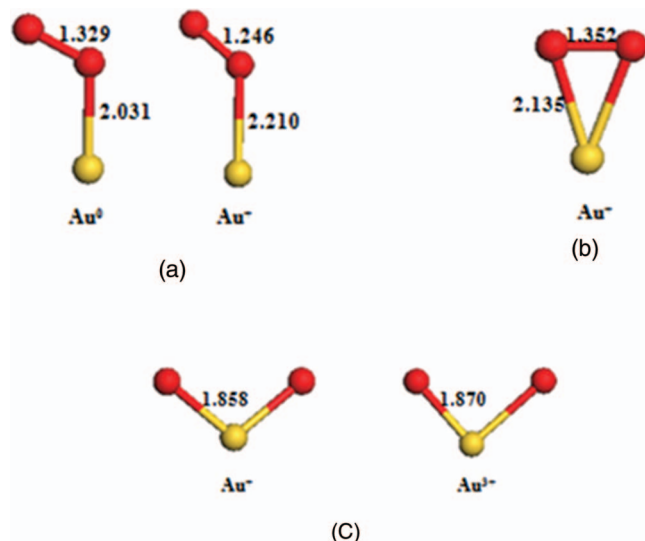


FIG. 2. Optimized structures of  $O_2$  adsorbed on gas phase neutral and charged Au atom. (a) Top coordination, (b) bridged coordination, and (c) dissociative coordination.

$Au^+-O_2$  as against 2.03 Å in  $Au^0-O_2$  (Table I). This can be inferred based on the fact that the Au–O bond is mostly electrostatic in nature in the former while being covalent (involving electron transfer) in the latter. The adsorbed  $O_2$  molecule is bent in both the cases with the Au–O–O bond angle increasing with increase in oxidation state ( $119.21^\circ$  in  $Au^0$  and  $130.98^\circ$  in  $Au^+$ ) (Table I).

In gas phase Au monomer,  $O_2$  adsorption in the bridge mode has been observed only on  $Au^+$  (Fig. 2(b)), not on  $Au^0$  and  $Au^{3+}$ ; while in the dissociative mode, adsorption is possible on both  $Au^+$  and  $Au^{3+}$  (Fig. 2(c)) but not on  $Au^0$ . However, both the bridge and dissociative modes of  $O_2$  adsorption on  $Au^+$  is unfavorable indicated by the negative binding energy, while in  $Au^{3+}$  positive binding energy indicates the dissociative adsorption to be favorable. In the bridge mode, the Au–O distance is found to be 2.14 Å while the O–O distance is 1.35 Å in  $Au^+$  (Table I). The Au–O distance in the dissociative mode is  $\sim 1.86$ – $1.87$  Å in both  $Au^+$  and  $Au^{3+}$ . It can be said that on gas phase  $Au^{3+}$ , of all the modes of  $O_2$  adsorption, only the dissociative adsorption is possible, in fact this occurs with a very high binding energy (4.86 eV). On

TABLE I. Computed selected geometrical parameters, binding energy and vibrational frequency of  $O_2$  adsorbed on gas phase neutral and charged gold monomer.

	Bond length (Å)		B.E (eV)	$\nu_{O-O}$ (cm <sup>-1</sup> )
	Au–O	O–O		
Top coordination				
Au <sup>0</sup> -O <sub>2</sub>	2.03	1.33	0.26	1067.1
Au <sup>+</sup> -O <sub>2</sub>	2.21	1.25	− 0.42	1441.7
Bridged coordination				
Au <sup>+</sup> -O <sub>2</sub>	2.14	1.35	− 0.89	1048.2
Dissociative coordination				
Au <sup>+</sup> -O <sub>2</sub>	1.86	2.89	− 3.84	...
Au <sup>3+</sup> -O <sub>2</sub>	1.87	2.85	4.68	...

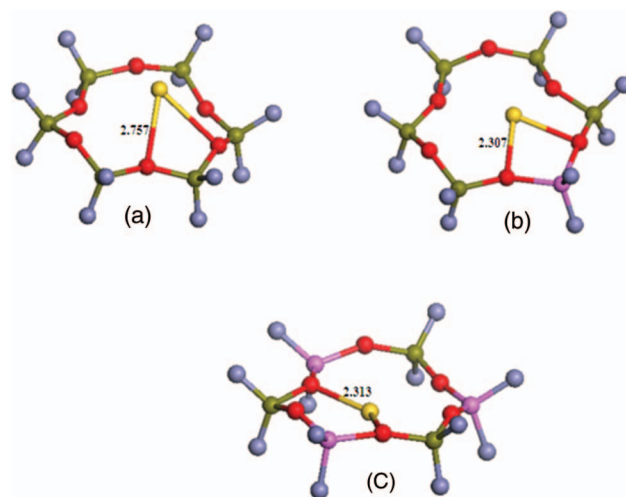


FIG. 3. Optimized structures of faujasite supported Au monomer; (a)  $Au^0/FAU$ , (b)  $Au^+/FAU$ , and (c)  $Au^{3+}/FAU$ , gray—H, red—O, green—Si, magenta—Al, and yellow—Au.

the other hand, bridge and dissociative  $O_2$  adsorption is not possible on  $Au^0$ ; however, adsorption is favorable in the top coordination. In the case of  $Au^+$ , although all the adsorption modes are possible, but these are accompanied by negative binding energy, making it unfavorable.

## B. $O_2$ adsorption over zeolite supported Au monomer

The optimized structures of faujasite supported Au monomer in three different oxidation states 0, +1, +3 are shown in Fig. 3. Selected geometrical parameters are summarized in Table II. The Au– $O_z$  ( $O_z$  represents framework zeolite oxygen) distance shows a decreasing trend on going from neutral to cationic clusters having a value of 2.31 Å for  $Au^{3+}$ . The Au–Si and Au–Al distances are observed to decrease with an increase in oxidation state. This suggests that the interaction of Au monomer with the faujasite support increases on moving to higher oxidation state. From the NBO charge analysis, it has been observed that anchoring of the Au monomer to the faujasite support causes a withdrawal of charge density from the zeolite to the monomer in both neutral and cationic systems evident from the charge carried by the Au monomer. For instance, the NBO charge for neutral Au has been found to be  $-0.06$  e while for the oxidation state of +1, the NBO charge on Au is 0.64 e.

First, we consider the case of  $O_2$  adsorbed in the top mode of coordination over faujasite supported gold monomer

TABLE II. Computed selected bond lengths (Å) and NBO charge on Au in faujasite supported bare Au monomer in three oxidation states 0, +1, +3.

	$Au^0/FAU$	$Au^+/FAU$	$Au^{3+}/FAU$
Bond length			
Au– $O_z$	2.75	2.30	2.31
Au–Si	3.32	2.98	2.97
Au–Al	...	3.08	2.96
Charge			
Q(Au)	–0.06	0.64	0.59

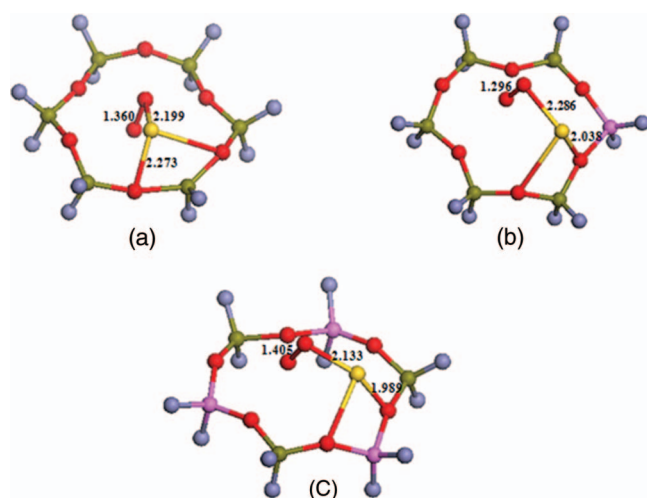


FIG. 4. Optimized structures of  $O_2$  adsorbed (top coordination) on faujasite supported Au monomer; (a)  $Au^0-O_2/FAU$ , (b)  $Au^+-O_2/FAU$ , and (c)  $Au^{3+}-O_2/FAU$ .

(Fig. 4). The Au–O bond distance reveals the interaction of the supported gold monomer with the adsorbed  $O_2$  molecule having the lowest value (2.13 Å) for  $Au^{3+}-O_2$  system indicating stronger interaction between Au monomer and  $O_2$ , while the highest bond distance (2.29 Å) has been observed for  $Au^+-O_2$  system that indicates the interaction to be weak. The Au–O distance for the neutral system is found to be intermediate of  $Au^{3+}$  and  $Au^+$  (2.19 Å in  $Au^0-O_2/FAU$ , Table III). For the O–O bond length the trend is just the opposite of the Au–O bond distance. The O–O bond is longest in faujasite supported  $Au^{3+}-O_2$  being 1.41 Å that approaches the O–O bond length in peroxide ion while in case of faujasite supported  $Au^0-O_2$  it decreases to 1.36 Å similar to the O–O bond distance in superoxide indicating  $O_2$  activation. However, in  $Au^+-O_2/FAU$ , the O–O bond length (1.29 Å) is comparable to that in free  $O_2$  (1.25 Å). The NBO charge on  $O_2$  bound to faujasite supported Au monomer is presented in Table IV. The  $\Delta q$  values represent the amount of charge transferred to the  $O_2$  molecule as a result of the interaction with the zeolite supported Au monomer. The highest  $\Delta q$  value of 0.47 e is observed for  $Au^0-O_2/FAU$  and the lowest value of 0.13 e for  $Au^+-O_2/FAU$ ; for  $Au^{3+}-O_2/FAU$   $\Delta q$  has an intermediate value. In  $Au^+-O_2/FAU$  the charge transferred is the lowest and consequently the O–O bond length has a value as that in free  $O_2$ . The  $\Delta q$  values indicate that charge is transferred

to  $O_2$  that goes to the antibonding orbital of  $O_2$  resulting in the lowering of the vibrational frequency of O–O bond. The  $\nu_{O-O}$  value increases from 916.3  $cm^{-1}$  in  $Au^{3+}-O_2/FAU$  to 1237.5  $cm^{-1}$  in  $Au^+-O_2/FAU$ ; being an intermediate value (1076.3  $cm^{-1}$ ) for  $Au^0-O_2/FAU$ . (The  $\nu_{O-O}$  value for free  $O_2$  is found to be 1436.1  $cm^{-1}$ ). The NBO charge on Au increases in case of  $Au^0$  and  $Au^{3+}$  on adsorption of  $O_2$  compared to that when  $O_2$  is absent also indicating charge transfer while it remains almost same in case of  $Au^+$ . The unchanged NBO charge on  $Au^+$  indicates that the interaction of  $Au^+$  and  $O_2$  is merely electrostatic in nature. The Au–O and O–O bond distances are indications of the interaction of faujasite supported Au monomer with the adsorbed  $O_2$  molecule. The shortest Au–O distance and the longest O–O distance in  $Au^{3+}-O_2/FAU$  can be attributed to the electron transfer from Au to  $O_2$ , when an extra electron goes to the antibonding orbital of  $O_2$  making O–O bond length longer. The interaction in case of  $Au^+-O_2/FAU$  is mostly weak electrostatic interaction in contrast to strong electron transfer interaction in  $Au^{3+}-O_2/FAU$ . The effect of the support can be evidenced from the fact that the adsorption of  $O_2$  on gas phase  $Au^{3+}$  is not possible, however, on zeolite supported  $Au^{3+}$ ,  $O_2$  gets activated. The shortest Au– $O_z$  ( $O_z$  represents the framework zeolite oxygen) has been found to be 2.27 Å in neutral Au monomer which decreases to 1.99 Å in  $Au^{3+}$  supported on faujasite zeolite. Decreasing bond length between Au and faujasite oxygen with increasing oxidation state indicates the increased interaction of the Au monomer with the support which favors the activation of  $O_2$  on faujasite supported Au monomer. However,  $O_2$  binding in the top mode to the faujasite supported Au monomer in all the three oxidation states is found to be unfavorable indicated by the negative binding energy value. A change in the zeolite–Au interaction in both the neutral and cationic systems has been observed as a consequence of  $O_2$  adsorption. The Au– $O_z$  distance in  $Au^0/FAU$  and  $Au^{3+}/FAU$  has a value of 2.75 Å and 2.31 Å, respectively, which decreases to 2.27 Å and 1.99 Å, respectively, when  $O_2$  is adsorbed on the Au monomer.

Unlike in the gas phase, the adsorption of  $O_2$  in the bridge mode is possible in both neutral and charged clusters (Fig. 5). For  $Au^0$  and  $Au^+$ , stable aggregates are obtained evident from the positive binding energy values. In fact,  $O_2$  binds to neutral Au in presence of faujasite support with a high binding energy of 1.63 eV while with a much lower value of 0.03 eV in  $Au^+$ . The adsorption, however, is accompanied by

TABLE III. Computed selected bond lengths (Å), binding energy (eV), and vibrational frequency of  $O_2$ ,  $\nu_{O-O}$  ( $cm^{-1}$ ) adsorbed on faujasite supported neutral and charged gold monomer.  $O_2$ (t)-top coordination,  $O_2$ (b)-bridged coordination,  $O_2$ (d)-dissociative coordination.

	$Au^0-O_2$ (t)/FAU	$Au^0-O_2$ (b)/FAU	$Au^0-O_2$ (d)/FAU	$Au^+-O_2$ (t)/FAU	$Au^+-O_2$ (b)/FAU	$Au^+-O_2$ (d)/FAU	$Au^{3+}-O_2$ (t)/FAU	$Au^{3+}-O_2$ (b)/FAU	$Au^{3+}-O_2$ (d)/FAU
Au–O	2.19	2.07	1.95	2.29	2.04	2.05	2.13	2.05	2.06
O–O	1.36	1.38	2.09	1.29	1.42	1.42	1.41	1.40	1.41
Au–Si	2.43	3.36	2.85	2.90	3.21	3.26	2.85	2.84	2.88
Au–Al	...	...	...	3.11	2.89	2.96	2.93	3.30	3.42
Au– $O_z$	2.27	2.71	2.40	2.04	2.14	2.28	1.99	2.26	2.31
$\nu_{O-O}$	1076.3	1062.2	600.3	1237.5	1034.8	1018.7	916.3	1040.5	1029.5
B.E	–1.56	1.63	–0.77	–0.85	0.03	0.34	–0.61	–0.13	0.04

TABLE IV. Computed NBO charges ( $Q$ ) and charge transferred ( $\Delta q$ ) in the different adsorption modes of  $O_2$  on faujasite supported Au monomer.

	$Au^0-O_2/FAU$			$Au^+-O_2/FAU$			$Au^{3+}-O_2/FAU$		
	Top	Bridged	Dissociative	Top	Bridged	Dissociative	Top	Bridged	Dissociative
$Q(Au)$	0.49	0.42	0.77	0.63	0.98	0.98	0.85	0.95	0.97
$Q(O)$	-0.24	-0.35	-0.52	-0.17	-0.26	-0.25	-0.27	-0.23	-0.23
$Q(O)$	-0.23	-0.18	-0.41	0.04	-0.25	-0.23	0.05	-0.21	-0.22
$\Delta q$	-0.47	-0.53	-0.93	-0.13	-0.51	-0.48	-0.21	-0.44	-0.45

a negative binding energy in case of  $Au^{3+}$ . The Au–O distance has a higher value of 2.07 Å in  $Au^0$  while it remains similar in  $Au^+$  and  $Au^{3+}$  ( $\sim 2.04$  Å). The O–O bond distance has a shorter value of 1.38 Å in  $Au^0$  in accordance with higher Au–O distance whereas a longer value of  $\sim 1.41$  Å in the cationic systems as a consequence of shorter Au–O distance. This indicates stronger interaction of  $O_2$  with the cationic Au compared to neutral Au (Table III). The corresponding vibrational frequency,  $\nu_{O-O}$  is lowered from that in free  $O_2$  with the highest value of 1062.2  $cm^{-1}$  for  $Au^0$  and almost similar lower value for  $Au^+$  and  $Au^{3+}$  ( $\sim 1040.5$   $cm^{-1}$ ). The NBO charge on  $O_2$  reveals transfer of charge ( $\Delta q$  value, Table IV) to  $O_2$  in all the three oxidation states. For  $Au^0$  and  $Au^+$ , about 0.5 e charge is transferred to  $O_2$  while a slightly lower amount in  $Au^{3+}$ . The O–O bond elongation might result from this charge transfer as a consequence of populating the antibonding orbital of  $O_2$ . The Au– $O_z$  distance ( $O_z$  represents framework zeolite oxygen) is observed to have a higher value for  $Au^0$  (2.71 Å) indicating less interaction with the support while shorter bond lengths in  $Au^+$  (2.14 Å) and  $Au^{3+}$  (2.26 Å) indicating increased interaction. However, in all the three oxidation states, the Au– $O_z$  distance in  $Au^n-O_2(b)/FAU$  ( $n = 0, +1, +3$ ) has a slightly lower value compared to that in faujasite supported bare monomer. An increase in the NBO charge on Au from  $-0.06$  e (in faujasite supported bare monomer) to 0.42 e (in  $O_2$  adsorbed faujasite supported monomer) in neu-

tral Au is observed as a result of  $O_2$  coordination in the bridge mode. Likewise, an increase from 0.64 e to 0.98 e and from 0.59 e to 0.95 e is observed in  $Au^+$  and  $Au^{3+}$ , respectively.

When the dissociative mode of  $O_2$  adsorption on faujasite supported Au monomer (Fig. 6) is considered the situation is different from the gas phase. Unlike in gas phase  $Au^0$ ,  $O_2$  adsorption is possible in faujasite supported neutral Au with Au–O bond length of 1.95 Å with the O atoms of  $O_2$  remaining far apart at a distance of 2.09 Å. The adsorption, however, is unfavorable evident from the negative binding energy of  $-0.77$  eV. In faujasite supported  $Au^+$  and  $Au^{3+}$ , the adsorption in dissociative mode is favorable, with faujasite supported  $Au^+$  possessing higher binding energy (0.34 eV) compared to  $Au^{3+}$ . It has been observed that the O atoms of  $O_2$  are at a distance of  $\sim 1.41$  Å in both  $Au^+$  and  $Au^{3+}$  approaching that in peroxide ion, or in other words, in faujasite supported cationic monomer,  $O_2$  prefers to remain in the peroxide form rather being dissociated. This can also be evidenced from the corresponding vibrational frequency,  $\nu_{O-O}$  given in Table III. In  $Au^0$ ,  $\nu_{O-O}$  has a much lower value of 600.3  $cm^{-1}$  while the value is almost similar for  $Au^+$  (1018.7  $cm^{-1}$ ) and  $Au^{3+}$  (1040.5  $cm^{-1}$ ). The NBO charge on  $O_2$  correlates with the observed O–O bond length. The amount of charge transferred to  $O_2$  is quite high in  $Au^0$  (0.93 e) compared to  $Au^+$  (0.48 e) and  $Au^{3+}$  (0.45 e) resulting in the O atoms of  $O_2$  to remain far apart in the neutral Au.

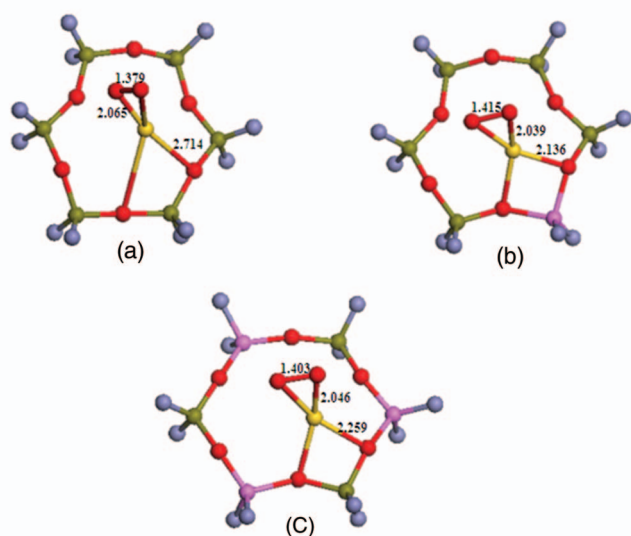


FIG. 5. Optimized structures of  $O_2$  adsorbed (bridge coordination) on faujasite supported Au monomer; (a)  $Au^0-O_2/FAU$ , (b)  $Au^+-O_2/FAU$ , and (c)  $Au^{3+}-O_2/FAU$ .

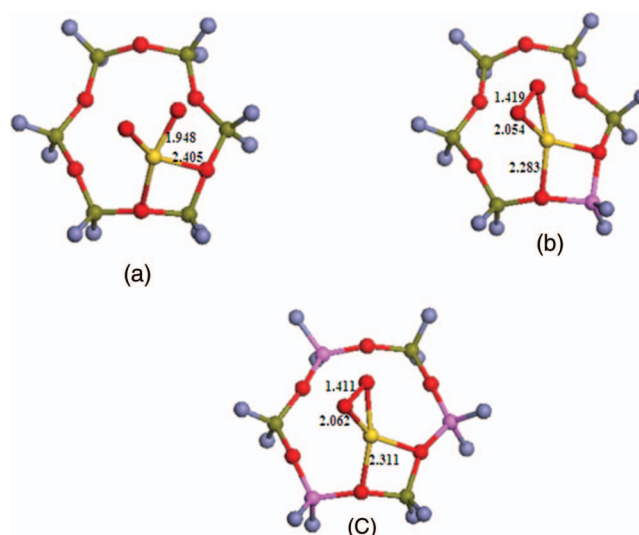


FIG. 6. Optimized structures of  $O_2$  adsorbed (dissociative coordination) on faujasite supported Au monomer; (a)  $Au^0-O_2/FAU$ , (b)  $Au^+-O_2/FAU$ , and (c)  $Au^{3+}-O_2/FAU$ .



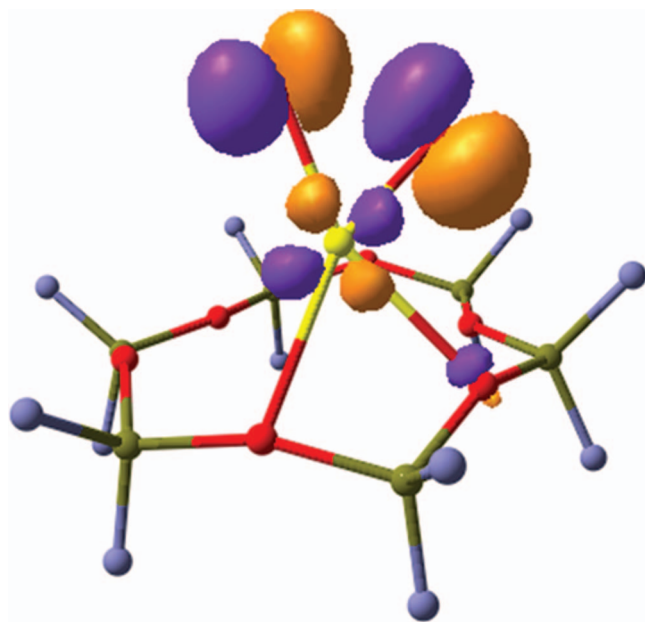


FIG. 7. HOMO-1 orbital of  $\text{Au}^0\text{-O}_2/\text{FAU}$  showing the  $\sigma^*$  occupancy of  $\text{O}_2$  and thus breaking the O–O bond.

NBO analysis of free gas phase  $\text{O}_2$  molecule shows zero occupancy of the  $\sigma^*$  and the  $\pi^*$  orbitals showing O=O double bond (1.25 Å). When  $\text{O}_2$  is adsorbed on  $\text{Au}^{3+}/\text{FAU}$  an increase in occupancy of the  $\pi^*$  orbital of  $\text{O}_2$  from 0 to 0.68540 is observed which contributes to the elongation of the O–O bond (1.41 Å) in  $\text{Au}^{3+}\text{-O}_2/\text{FAU}$  approaching the O–O bond of a peroxide species. NBO analysis on  $\text{Au}^+\text{-O}_2/\text{FAU}$  system shows a slight increase in occupancy of  $\sigma^*$  orbital of  $\text{O}_2$  from 0 to 0.00329 resulting further elongation of O–O bond (1.42 Å). In the case of  $\text{Au}^0\text{-O}_2/\text{FAU}$  no O–O bond is found due to occupancy of the  $\sigma^*$  orbital of  $\text{O}_2$ . The HOMO-1 orbital showing the occupancy of  $\sigma^*$  orbital and thus breaking the O–O bond which is shown in Fig. 7. When  $\text{O}_2$  is coordinated in dissociative mode, the NBO charge on Au increases from  $-0.06$  e in faujasite supported bare  $\text{Au}^0$  to 0.77 e in  $\text{O}_2$  adsorbed  $\text{Au}^0/\text{FAU}$ . In the case of  $\text{Au}^+$  and  $\text{Au}^{3+}$ , it increases from 0.63 e to 0.98 e and from 0.59 e to 0.97 e, respectively. Comparing the NBO charge on Au when  $\text{O}_2$  is adsorbed in the bridge and dissociative mode, we find that the increase in charge from the value in faujasite supported bare monomer is almost similar in both  $\text{Au}^+$  and  $\text{Au}^{3+}$  which might result in the similar elongation of O–O bond length. This is indicated by the O–O bond length (Table III) that approaches the value in peroxide ( $\sim 1.40\text{--}1.42$  Å) in both the oxidation states for the two adsorption modes. However, the increase is quite high for the dissociative mode compared to the bridge mode in neutral Au and consequently higher amount of charge is transferred from Au in the former mode. This is evident from the O–O bond distance in both the adsorption modes in  $\text{Au}^0/\text{FAU}$ , being much higher in the dissociative mode. In  $\text{Au}^0/\text{FAU}$ , Au–O distance has a lower value of 1.95 Å while similar values are observed in  $\text{Au}^+/\text{FAU}$  and  $\text{Au}^{3+}/\text{FAU}$ . The Au– $\text{O}_z$  distance is almost similar in both the cationic states. However, the Au– $\text{O}_z$  distance is found to decrease from 2.76 Å in faujasite supported bare  $\text{Au}^0$  to 2.40 Å in  $\text{O}_2$  adsorbed faujasite

supported  $\text{Au}^0$ . On the other hand, the decrease is observed to be slightly less in  $\text{Au}^+$  (from 2.31 Å to 2.28 Å) and in  $\text{Au}^{3+}$  the Au– $\text{O}_z$  distance remains same.

#### IV. CONCLUSIONS

Our study on  $\text{O}_2$  adsorption on faujasite supported Au monomer in three different oxidation states (0, +1, +3) reveals activation of  $\text{O}_2$  indicated by the elongation of O–O bond length and corresponding redshift in the  $\nu_{\text{O-O}}$  from the value in gas phase free  $\text{O}_2$ . Activation of  $\text{O}_2$  is an important step in the catalytic oxidation of CO. It has been observed that the  $\text{O}_2$  binding in the top mode is accompanied by negative binding energy value in all the three oxidation states making it unfavorable. In neutral Au,  $\text{O}_2$  binding, however, is favorable in the bridge coordination with a high binding energy. On the other hand, in faujasite supported cationic Au,  $\text{O}_2$  reverts back to the bridge bonded form rather than being dissociated. However, the presence of  $\text{O}_2$  facilitates the interaction of Au monomer with the faujasite support evident from reduced Au– $\text{O}_z$  distances.

#### ACKNOWLEDGMENTS

The authors thank the Department of Science and Technology, New Delhi for financial support.

- <sup>1</sup>M. Haruta, T. Kobayashi, H. Samo, and N. Yamada, *Chem. Lett.* **2**, 405 (1987).
- <sup>2</sup>M. Haruta, N. Yamada, T. Kobayashi, and S. Ijima, *J. Catal.* **115**, 301 (1989).
- <sup>3</sup>M. Haruta, S. Tsubota, T. Kobayashi, H. Kageyama, M. J. Genet, and B. Delmon, *J. Catal.* **144**, 175 (1993).
- <sup>4</sup>Q. Fu, H. Saltaburg, and M. F. Stephanopoulos, *Science* **301**, 935 (2003).
- <sup>5</sup>A. Corma and P. Serna, *Science* **313**, 332 (2006).
- <sup>6</sup>M. D. Hughes, Y. J. Xu, P. Jenkins, P. McMorn, P. Landon, D. I. Enache, A. F. Carley, G. A. Attard, G. J. Hutchings, F. King, E. H. Stitt, P. Johnston, K. Griffin, and C. J. Kiely, *Nature* **437**, 1132 (2005).
- <sup>7</sup>M. Turner, V. B. Golovko, O. P. H. Vaughan, P. Abdulkhan, A. Berenguer-Murcia, M. S. Tikhov, B. F. G. Johnson, and R. M. Lambert, *Nature* **454**, 981 (2008).
- <sup>8</sup>D. M. Cox, R. O. Brickman, K. Creegan, and A. Kaldor, *Z. Phys. D: At. Mol. Clusters* **19**, 353 (1991).
- <sup>9</sup>D. M. Cox, R. O. Brickman, K. Creegan, and A. Kaldor, *Mater. Res. Soc. Symp. Proc.* **206**, 43 (1991).
- <sup>10</sup>B. E. Salisbury, W. T. Wallace, and R. L. Whetten, *Chem. Phys.* **262**, 131 (2000).
- <sup>11</sup>W. T. Wallace and R. L. Whetten, *J. Am. Chem. Soc.* **124**, 7499 (2002).
- <sup>12</sup>J. Hagen, L. D. Socaciu, M. Eljazyfer, U. Heiz, T. M. Bernhardt, and L. Woste, *Phys. Chem. Chem. Phys.* **4**, 1707 (2002).
- <sup>13</sup>D. Stolcic, M. Fischer, G. Gantefor, Y. D. Kim, Q. Sun, and P. Jena, *J. Am. Chem. Soc.* **125**, 2848 (2003).
- <sup>14</sup>W. T. Wallace, A. J. Leavitt, and R. L. Whetten, *Chem. Phys. Lett.* **368**, 774 (2003).
- <sup>15</sup>G. Mills, M. S. Gordon, and H. Metiu, *J. Chem. Phys.* **118**, 4198 (2003).
- <sup>16</sup>X. Ding, Z. Li, J. Yang, J. G. Hou, and Q. Zhu, *J. Chem. Phys.* **120**, 9594 (2004).
- <sup>17</sup>B. Yoon, H. Häkkinen, and U. Landman, *J. Phys. Chem. A* **107**, 4066 (2003).
- <sup>18</sup>L. M. Molina, M. D. Rasmussen, and B. Hammer, *J. Chem. Phys.* **120**, 7673 (2004).
- <sup>19</sup>Y. Xu and M. Mavrikakis, *J. Phys. Chem. B* **107**, 9298 (2003).
- <sup>20</sup>M. Okumura, M. Haruta, Y. Kitagawa, and K. Yamaguchi, *Gold Bull.* **1**, 40 (2007).
- <sup>21</sup>A. Roldán, J. M. Ricart, F. Illas, and G. Pacchioni, *Phys. Chem. Chem. Phys.* **12**, 10723 (2010).



- <sup>22</sup>M. Okumura, Y. Kitagawa, M. Haruta, K. Yamaguchi, *Chem. Phys. Lett.* **346**, 163 (2001).
- <sup>23</sup>Y-Ping Xie and X-Gao Gong, *J. Chem. Phys.* **132**, 244302 (2010).
- <sup>24</sup>A. Prestianni, A. Martorana, F. Labat, I. Ciofini, and C. Adamo, *J. Phys. Chem. B* **110**, 12240 (2006).
- <sup>25</sup>S. Qiu, R. Ohnishi, and M. Ichikawa, *J. Chem. Soc., Chem. Commun.* **19**, 1425 (1992).
- <sup>26</sup>J. C. Fierro-Gonzalez and B. C. Gates, *J. Phys. Chem. B* **108**, 16999 (2004).
- <sup>27</sup>T. M. Salama, T. Shido, R. Ohnishi, and M. Ichikawa, *J. Chem. Soc., Chem. Commun.* 2749 (1994).
- <sup>28</sup>M. M. Mohammed, T. M. Salama, and M. Ichikawa, *J. Colloid Interface Sci.* **224**, 366 (2000).
- <sup>29</sup>M. M. Mohammed and M. Ichikawa, *J. Colloid Interface Sci.* **232**, 381 (2000).
- <sup>30</sup>S. Qiu, R. Ohnishi, and M. Ichikawa, *J. Phys. Chem.* **98**, 2719 (1994).
- <sup>31</sup>Z. Gao, Q. Sun, H. Chen, X. Wang, and W. M. H. Sachtler, *Catal. Lett.* **72**, 1 (2001).
- <sup>32</sup>A. N. Pestryakov, N. Bogdanchikova, A. Simakov, I. Tuzovskaya, F. Jentoft, M. Farias, and A. Diaz, *Surf. Sci.* **601**, 3792 (2007).
- <sup>33</sup>A. N. Pestryakov, I. Tuzovskaya, E. Smolentseva, N. Bogdanchikova, F. Jentoft, and A. Knop-gericke, *Int. J. Mod. Phys. B* **19**, 2321 (2005).
- <sup>34</sup>I. Tuzovskaya, A. Simakov, A. N. Pestryakov, N. Bogdanchikova, V. V. Gurin, M. Farias, H. J. Tiznado, and M. Avalos, *Catal. Commun.* **8**, 977 (2007).
- <sup>35</sup>N. Lopez and J. K. Nørskov, *J. Am. Chem. Soc.* **124**, 11262 (2002).
- <sup>36</sup>T. Jiang, D. J. Mowbray, S. Dobrin, H. Falsig, B. Hvolbaek, T. Bligaard, and J. K. Nørskov, *J. Phys. Chem. C* **113**, 10548 (2009).
- <sup>37</sup>A. Roldan, S. Gonzalez, J. M. Ricart, and F. Illas, *ChemPhysChem* **10**, 348 (2009).
- <sup>38</sup>M. Boronat and A. Corma, *Dalton Trans.* **39**, 8538 (2010).
- <sup>39</sup>J. R. Shoemaker, L. W. Burggraf, and M. S. Gordon, *J. Phys. Chem. A* **103**, 3245 (1999).
- <sup>40</sup>M. J. Frisch, G. W. Trucks, H. B. Schlegel *et al.*, GAUSSIAN 09, Revision A.1, Gaussian, Inc., Wallingford, CT, 2009.